Tensor to scalar ratio in nonminimal φ^4 inflation

Nobuchika Okada,[1,*] Mansoor Ur Rehman,[2,†] and Qaisar Shafi[2,‡]

[1]*Department of Physics and Astronomy, University of Alabama, Tuscaloosa, Alabama 35487, USA*
[2]*Bartol Research Institute, Department of Physics and Astronomy, University of Delaware, Newark, Delaware 19716, USA*

We reconsider nonminimal $\lambda\phi^4$ chaotic inflation which includes the gravitational coupling term $\xi\mathcal{R}\phi^2$, where ϕ denotes a gauge singlet inflaton field and $\mathcal{R}$ is the Ricci scalar. For $\xi \gg 1$, we require, following recent discussions, that the energy scale $\lambda^{1/4}m_P/\sqrt{\xi}$ for inflation should not exceed the effective UV cutoff scale m_P/ξ, where m_P denotes the reduced Planck scale. The predictions for the tensor-to-scalar ratio r and the scalar spectral index n_s are found to lie within the Wilkinson Microwave Anisotropy Probe 1-σ bounds for $10^{-12} \lesssim \lambda \lesssim 10^{-4}$ and $10^{-3} \lesssim \xi \lesssim 10^2$. In contrast, the corresponding predictions of minimal $\lambda\phi^4$ chaotic inflation lie outside the Wilkinson Microwave Anisotropy Probe 2-σ bounds. We also find that $r \gtrsim 0.002$, provided the scalar spectral index $n_s \gtrsim 0.96$. In estimating the lower bound on r, we take into account possible modifications due to quantum corrections of the tree level inflationary potential.

PACS numbers: 98.80.Cq

The idea that the inflaton may be a scalar field having an additional nonminimal coupling to gravity has received a fair amount of attention [1–10]. In one of the simplest scenarios of this kind, the standard model (SM) Higgs doublet H has a relatively strong nonminimal gravitational interaction $\xi\mathcal{R}H^\dagger H$, where $\mathcal{R}$ is the Ricci scalar and ξ a dimensionless coupling whose magnitude is estimated to be of order 10^3–10^4 based on measurements by the Wilkinson Microwave Anisotropy Probe (WMAP) [11] and other cosmic microwave background anisotropy experiments. This SM Higgs based inflationary scenario is currently mired in some controversy stemming from arguments first put forward in [12] that for $\xi \gg 1$, the energy scale $\lambda^{1/4}m_P/\sqrt{\xi}$ during nonminimal SM inflation exceeds the effective ultraviolet cutoff scale $\Lambda = m_P/\xi$. Here λ of order unity denotes the SM Higgs quartic coupling and $m_P \simeq 2.43 \times 10^{18}$ GeV represents the reduced Planck mass. Thus, the "flat" region of the effective potential lies beyond the region of applicability of the naive approximation, and so there is no compelling reason to trust the purported inflationary phase [12–14]. For a different viewpoint see Ref. [15].

In this paper we reconsider nonminimal $\lambda\phi^4$ inflation and begin by replacing the SM Higgs inflaton with a gauge singlet scalar field. (The radial component of the axion field provides a nice example of a gauge singlet field and axion physics also provides a viable dark matter candidate.) We impose from the outset the requirement that the energy scale of inflation should not exceed the effective cutoff scale Λ. We also take into account quantum corrections to the inflationary potential arising from the interactions of the inflaton with other fields. Since one of our main

goals is to obtain a lower bound on r, we only include corrections arising from the Yukawa interactions which can decrease r. We find that $r \gtrsim 0.002$, provided the scalar spectral index $n_s \gtrsim 0.96$. More generally, in this nonminimal $\lambda\phi^4$ inflation model, the predictions for n_s and r lie within the WMAP 1-σ bounds for $10^{-12} \lesssim \lambda \lesssim 10^{-4}$ and $10^{-3} \lesssim \xi \lesssim 10^2$. Recall that the corresponding tree level predictions for minimal ($\xi = 0$) $\lambda\phi^4$ chaotic inflation, namely, $n_s \simeq 0.95$ and $r \simeq 0.26$, lie outside the WMAP 2-σ bounds.

We begin with the following tree level action in the Jordan frame:

$$S_J^{\text{tree}} = \int d^4x \sqrt{-g}\Bigg[-\left(\frac{m_P^2 + \xi\phi^2}{2}\right)\mathcal{R} + \frac{1}{2}(\partial\phi)^2 - \frac{\lambda}{4!}\phi^4 - \frac{1}{2}y_N\phi\bar{N}^cN \Bigg], \tag{1}$$

where ϕ is a gauge singlet scalar field and λ is the scalar self-coupling. In order to keep the discussion simple, we have introduced only a single right-handed neutrino N with Yukawa coupling y_N, and we ignore the bare mass term for N. In a more realistic scenario, at least two right-handed neutrinos are required for successful leptogenesis and reproducing neutrino oscillation data.

Using standard techniques [16], the one-loop renormalization group improved effective action can be written as

$$S_J = \int d^4x \sqrt{-g}\Bigg[-\left(\frac{m_P^2 + \xi\phi^2}{2}\right)\mathcal{R} + \frac{1}{2}(\partial\phi)^2 - \frac{1}{4!}\lambda(t)G(t)^4\phi^4 \Bigg], \tag{2}$$

where $t = \ln(\phi/\mu)$ and $G(t) = \exp(-\int_0^t dt'\gamma(t')/(1 + \gamma(t')))$, with $\gamma(t) = \frac{y_N^2}{(4\pi)^2}$ being the anomalous dimension of the inflaton field. We ignore quantum corrections to the

---

*okadan@ua.edu
†rehman@udel.edu
‡shafi@bartol.udel.edu

classical kinetic and gravity sectors in the above action [3,4]. Moreover, as the inflaton is a gauge singlet field in our case, we only need to consider the renormalization group equations of λ and y_N:

$$\frac{d\lambda}{dt} = \frac{1}{(4\pi)^2}(3\lambda^2 + 4\lambda y_N^2 - 24y_N^4), \tag{3}$$

$$\frac{dy_N}{dt} = \frac{1}{(4\pi)^2}\left(\frac{5}{4}y_N^3\right). \tag{4}$$

The requirement that the energy scale of inflation should lie below the cutoff scale ($\Lambda = m_P/\xi$ for $\xi \geq 1$ and $\Lambda = m_P$ for $\xi \leq 1$) generates values of the above couplings small enough to suppress the running of ξ. Therefore, we ignore the running of ξ in our numerical calculations.

In the Einstein frame with a canonical gravity sector, the kinetic energy can be made canonical with respect to a new field σ [4],

$$\left(\frac{d\sigma}{d\phi}\right)^{-2} = \frac{(1 + \frac{\xi\phi^2}{m_P^2})^2}{1 + (6\xi + 1)\frac{\xi\phi^2}{m_P^2}}. \tag{5}$$

The action in the Einstein frame is then given by

$$S_E = \int d^4x\sqrt{-g_E}\left[-\frac{1}{2}m_P^2\mathcal{R}_E + \frac{1}{2}(\partial_E\sigma)^2 - V_E(\sigma(\phi))\right], \tag{6}$$

with

$$V_E(\phi) = \frac{\frac{1}{4!}\lambda(t)G(t)^4\phi^4}{(1 + \frac{\xi\phi^2}{m_P^2})^2}. \tag{7}$$

To discuss things qualitatively it is convenient to use the following approximate form of the above potential:

$$V_E(\phi) = \frac{\frac{1}{4!}\lambda\phi^4 - \kappa\phi^4 \ln(\phi/\mu)}{(1 + \frac{\xi\phi^2}{m_P^2})^2}, \tag{8}$$

where we have assumed $\gamma \approx 0$, $dy_N/dt \approx 0$, $\lambda \ll y_N^2$, and $d\lambda/dt \approx -24\kappa$ with $\kappa = y_N^4/(4\pi)^2$. We have checked that in the relevant parametric region the above potential can be considered as a valid approximation. In our numerical calculations we fix the renormalization scale μ equal to the cutoff scale Λ.

Before starting our discussion of this model it is useful to recall here the basic results of the slow-roll assumption. The inflationary slow-roll parameters are given by

$$\epsilon(\phi) = \frac{1}{2}m_P^2\left(\frac{V_E'}{V_E\sigma'}\right)^2, \tag{9}$$

$$\eta(\phi) = m_P^2\left[\frac{V_E''}{V_E(\sigma')^2} - \frac{V_E'\sigma''}{V_E(\sigma')^3}\right], \tag{10}$$

$$\zeta^2(\phi) = m_P^4\left(\frac{V_E'}{V_E\sigma'}\right)\left(\frac{V_E'''}{V_E(\sigma')^3} - 3\frac{V_E''\sigma''}{V_E(\sigma')^4}\right.$$
$$\left. + 3\frac{V_E'(\sigma'')^2}{V_E(\sigma')^5} - \frac{V_E'\sigma'''}{V_E(\sigma')^4}\right), \tag{11}$$

where a prime denotes a derivative with respect to ϕ. The slow-roll approximation is valid as long as the conditions $\epsilon \ll 1$, $|\eta| \ll 1$, and $\zeta^2 \ll 1$ hold. In this case, the scalar spectral index n_s, the tensor-to-scalar ratio r, and the running of the spectral index $\frac{dn_s}{d\ln k}$ are approximately given by

$$n_s \simeq 1 - 6\epsilon + 2\eta, \tag{12}$$

$$r \simeq 16\epsilon, \tag{13}$$

$$\frac{dn_s}{d\ln k} \simeq 16\epsilon\eta - 24\epsilon^2 - 2\zeta^2. \tag{14}$$

The number of e-folds after the comoving scale l has crossed the horizon is given by

$$N_l = \frac{1}{\sqrt{2}m_P}\int_{\phi_e}^{\phi_l}\frac{d\phi}{\sqrt{\epsilon(\phi)}}\left(\frac{d\sigma}{d\phi}\right), \tag{15}$$

where ϕ_l is the field value at the comoving scale l, and ϕ_e denotes the value of ϕ at the end of inflation, defined by $\max(\epsilon(\phi_e), |\eta(\phi_e)|, \zeta^2(\phi_e)) = 1$.

The amplitude of the curvature perturbation $\Delta_\mathcal{R}$ is given by

$$\Delta_\mathcal{R}^2 = \frac{V_E}{24\pi^2m_P^4\epsilon}\bigg|_{k_0}, \tag{16}$$

where $\Delta_\mathcal{R}^2 = (2.43 \pm 0.11) \times 10^{-9}$ is the WMAP7 normalization at $k_0 = 0.002$ Mpc^{-1} [11]. Note that, for added precision, we include in our calculations the first order corrections [17] in the slow-roll expansion for the quantities n_s, r, $\frac{dn_s}{d\ln k}$, and $\Delta_\mathcal{R}$.

Using Eqs. (8)–(16) above we can obtain various predictions of the radiatively corrected nonminimal ϕ^4 model of inflation. Once we fix the parameters ξ and κ, and the number of e-foldings N_0, we can predict n_s, r, and $\frac{dn_s}{d\ln k}$. The tree level ($\kappa = 0$) minimal ϕ^4 predictions are readily obtained as

$$n_s = 1 - \frac{24}{\phi^2} = 1 - \frac{3}{N_0}, \tag{17}$$

$$r = \frac{128}{\phi^2} = \frac{16}{N_0}, \tag{18}$$

$$\frac{dn_s}{d\ln k} = -\frac{192}{\phi^4} = -\frac{3}{N_0^2}. \tag{19}$$

For $N_0 = 60$, we find $n_s \simeq 0.95$, $r \simeq 0.26$ and $\frac{dn_s}{d\ln k} \simeq -8 \times 10^{-3}$. As we mentioned above, this shows that the predic-
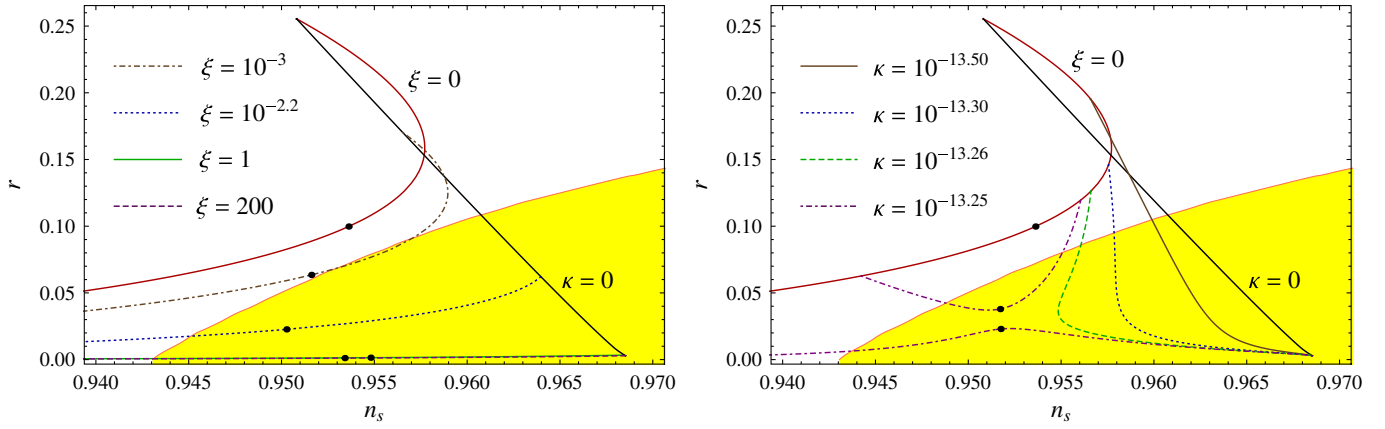
FIG. 1 (color online). r vs n_s for the radiatively corrected nonminimal ϕ^4 potential defined in Eq. (8) with the number of e-foldings $N_0 = 60$. The WMAP 1-σ (68% confidence level) bounds are shown in yellow. Along each curve we vary either κ (left panel) or ξ (right panel), keeping one or the other fixed. The black dots represent the meeting points of the hilltop and the ϕ^4 solutions and correspond, for a given ξ, to the maximum value of κ.

tions of tree level minimal ϕ^4 inflation lie outside the 2-σ WMAP bounds [11]. However, the situation improves once we include the radiative corrections [18] generated from the Yukawa interaction in Eq. (1). Recently, these radiative corrections have been shown to have important effects on the tree level predictions of various inflationary models [19,20]. The scalar spectral index, the tensor-to-scalar ratio and the running of the spectral index for the radiatively corrected minimal ϕ^4 inflation are then given by

$$n_s \simeq 1 - \left(2\left(\frac{1 - 78\kappa/\lambda}{1 - 72\kappa/\lambda}\right)^2 - \left(\frac{1 - 86\kappa/\lambda}{1 - 72\kappa/\lambda}\right)\right)\frac{3}{N_0}, \quad (20)$$

$$r \simeq \left(\frac{1 - 78\kappa/\lambda}{1 - 72\kappa/\lambda}\right)^2 \frac{16}{N_0}, \quad (21)$$

$$\frac{dn_s}{d\ln k} \simeq -\frac{3}{N_0^2}\left(\frac{(1 - 98\kappa/\lambda)(1 - 78\kappa/\lambda)}{(1 - 72\kappa/\lambda)^2}\right) + \frac{r}{2}\left(\frac{16r}{3} - (1 - n_s)\right). \quad (22)$$

The predicted values of n_s and r are shown in Figs. 1–3 for $N_0 = 60$ e-foldings. The running of the spectral index $\frac{dn_s}{d\ln k}$ varies from -3×10^{-3} to -8×10^{-3}. Although with the inclusion of radiative corrections we obtain a reduction in r, the predictions of the radiatively corrected minimal ϕ^4 inflation remain outside of the WMAP 1-σ bounds. If we take κ and the ratio κ/λ as our two independent parameters (instead of κ and λ), the value of κ can be easily obtained in terms of κ/λ and N_0 by employing Eq. (16):

$$\kappa \simeq \frac{(3\pi\Delta_{\mathcal{R}})^2}{N_0^3}\frac{(\kappa/\lambda)(1 - 78\kappa/\lambda)^2}{(1 - 72\kappa/\lambda)^3}. \quad (23)$$
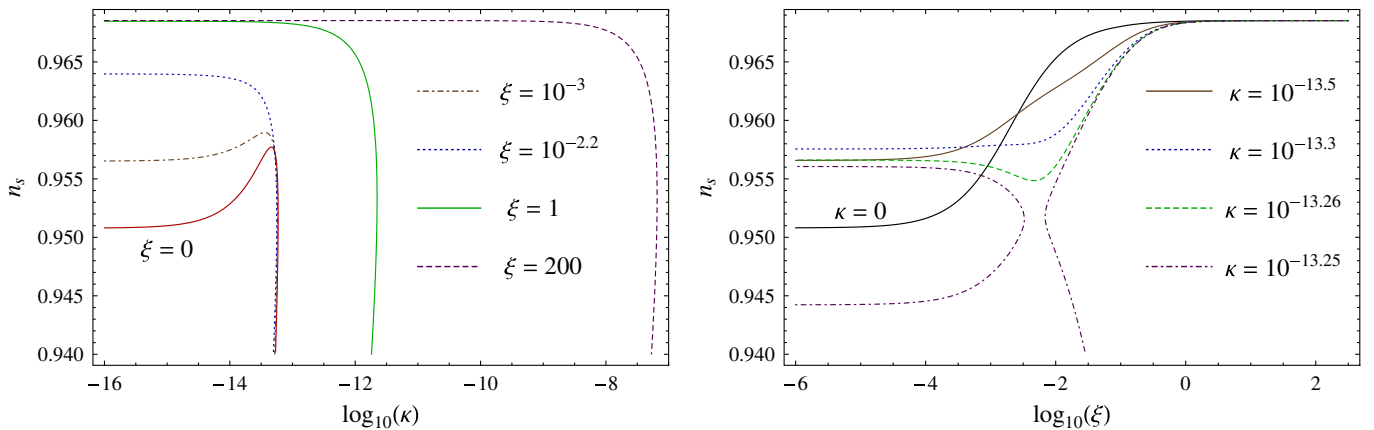

FIG. 2 (color online). n_s vs $\log_{10}(\kappa)$ and $\log_{10}(\xi)$ for radiatively corrected nonminimal ϕ^4 inflation with the number of e-foldings $N_0 = 60$.
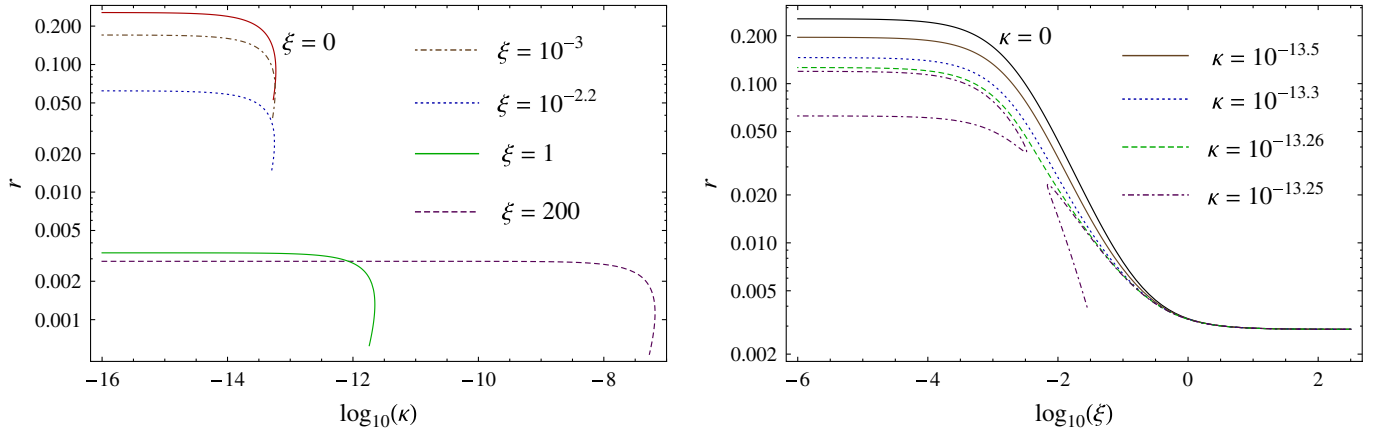
FIG. 3 (color online). r vs $\log_{10}(\kappa)$ and $\log_{10}(\xi)$ for radiatively corrected nonminimal ϕ^4 inflation with the number of e-foldings $N_0 = 60$.

The positive semidefinite condition $V \geq 0$ for the potential implies $\kappa/\lambda \leq 1/(24 \ln(\phi/m_P)) \simeq 1/72$. However, the WMAP 1-$\sigma$ bounds of the spectral index n_s impose a more stringent bound $\kappa/\lambda \lesssim 1/79$. It is interesting to note that the above result allows two solutions for each of κ/λ, n_s and r for a given value of κ [18]. These two solutions meet at $\kappa/\lambda \sim 1/90$ and correspond to the maximum value

of $\kappa \sim 10^{-13.6}$ as represented by the black dots in Fig. 1 and can be seen explicitly in Figs. 3 and 4. Following Ref. [18] we call the small κ/λ solution the "ϕ^4 solution" and the other the "hilltop solution." This hilltop solution mostly lies on the concave downward part of the potential, i.e., above the point of inflection whereas the ϕ^4 solution lies below the point of inflection. Moreover, the value of
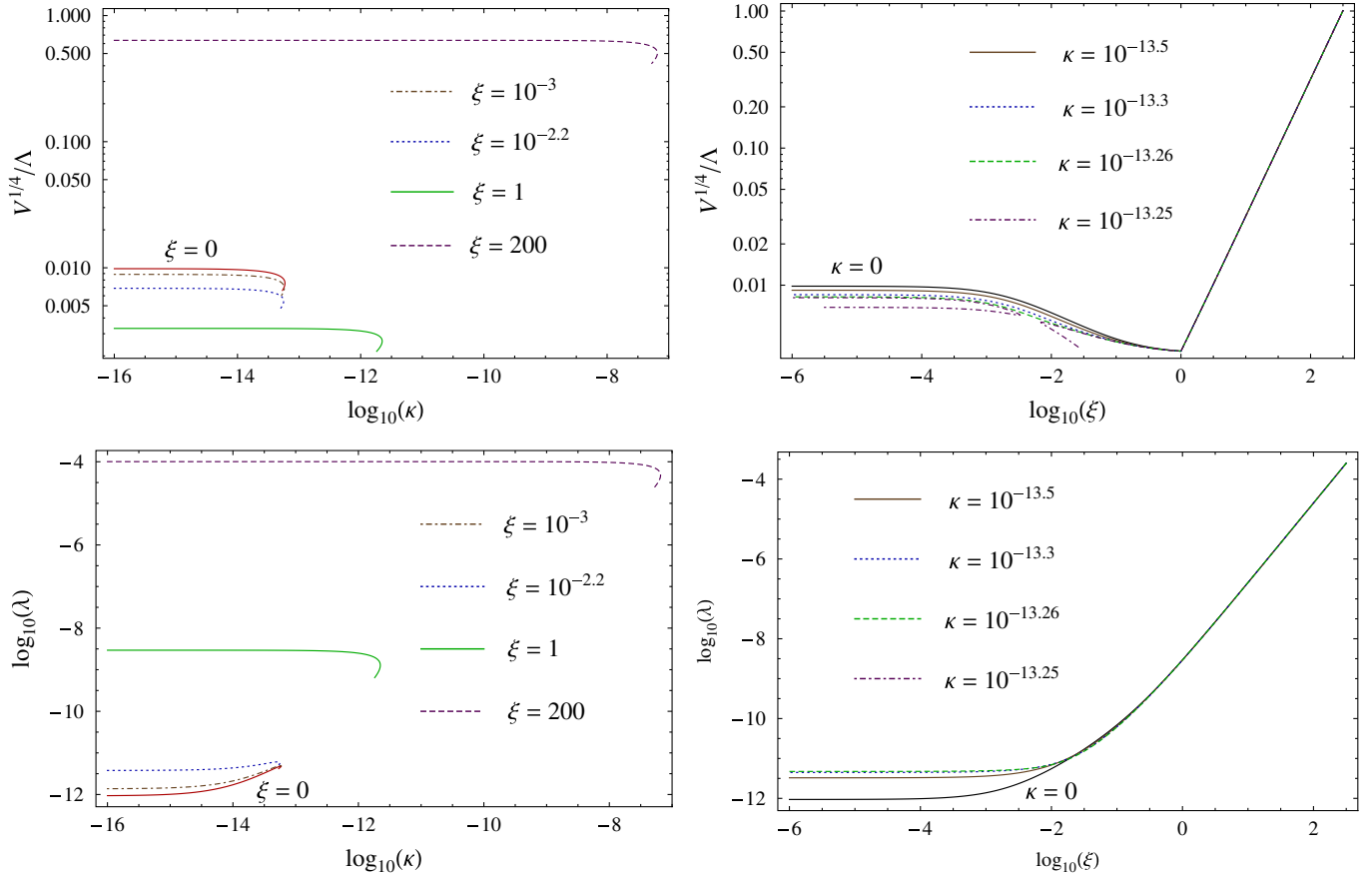

FIG. 4 (color online). $V^{1/4}/\Lambda$ and $\log_{10}(\lambda)$ vs $\log_{10}(\xi)$ and $\log_{10}(\kappa)$ for radiatively corrected nonminimal ϕ^4 inflation with the number of e-foldings $N_0 = 60$.

the inflaton field at the pivot scale ϕ_0 remains below the position of the hilltop in the WMAP 1-σ region. In this paper we mainly restrict our discussion to the WMAP 1-σ bounds.

For $\xi \neq 0$ and in the limit $\xi \ll 1$, the tree level predictions of minimal ϕ^4 inflation are modified as follows [21]:

$$n_s \simeq 1 - \frac{3(1 + 16\xi N_0/3)}{N_0(1 + 8\xi N_0)}, \qquad (24)$$

$$r \simeq \frac{16}{N_0(1 + 8\xi N_0)}, \qquad (25)$$

$$\frac{dn_s}{d\ln k} \simeq -\frac{3(1 + 4(8\xi N_0)/3 - 5(8\xi N_0)^2 - 2(8\xi N_0)^3)}{N_0^2(1 + 8\xi N_0)^4}$$
$$+ \frac{r}{2}\left(\frac{16r}{3} - (1 - n_s)\right). \qquad (26)$$

These results exhibit a reduction in the value of r and an increase in the value of n_s as can be seen in Figs. 1–3. In

particular, from the WMAP 1-σ bounds ($r \sim 0.1$ and $n_s \sim 0.96$), we obtain a lower bound of $\xi \gtrsim 3 \times 10^{-3}$ with $N_0 = 60$ e-foldings [2,21]. The tree level prediction for $\frac{dn_s}{d\ln k}$ receives only a tiny correction in this case. Note the sharp transitions in the predictions of n_s and r in the vicinity of $\xi \approx 10^{-2}$. This can be understood from the expression for the inflationary potential given in Eq. (8), (24), and (25).

In order to discuss nonminimal ϕ^4 inflation for $\xi \gg 1$, it is useful to define the dimensionless field variable $\psi \equiv \sqrt{\xi}\phi/m_P$. With $\xi, \psi \gg 1$, the tree level predictions for n_s, r and $\frac{dn_s}{d\ln k}$ are given by

$$n_s \simeq 1 - \frac{8}{3\psi^2} = 1 - \frac{2}{N_0}, \qquad (27)$$

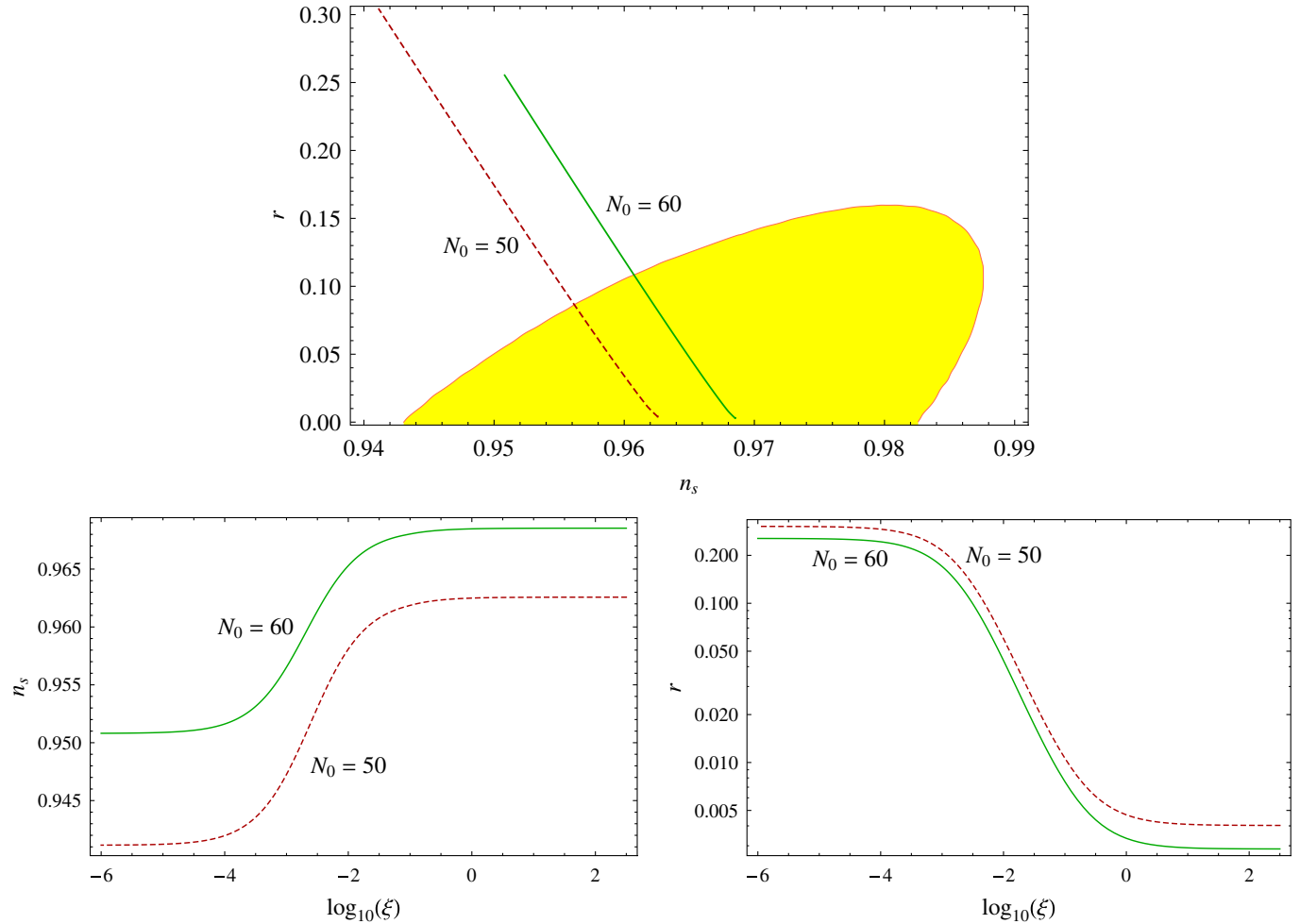$$r \simeq \frac{64}{3\psi^4} = \frac{12}{N_0^2}, \qquad (28)$$

FIG. 5 (color online). r vs n_s (first row) and n_s and r vs $\log_{10}(\xi)$ (second row) for tree level ($\kappa = 0$) nonminimal ϕ^4 inflation with the number of e-foldings $N_0 = 50$ (red dashed curve) and $N_0 = 60$ (green solid curve). The WMAP 1-σ (68% confidence level) bounds are shown in yellow.

$$\frac{dn_s}{d\ln k} \simeq -\frac{32}{9\psi^4} = -\frac{2}{N_0^2}, \qquad (29)$$

with

$$\Delta_{\mathcal{R}}^2 \simeq \frac{\lambda}{\xi^2}\left(\frac{\psi^4}{768\pi^2}\right) \simeq \frac{\lambda}{\xi^2}\left(\frac{N_0^2}{432\pi^2}\right). \qquad (30)$$

The results are shown as a black curve in Figs. 1–3 labeled $\kappa = 0$. The running of the spectral index $\frac{dn_s}{d\ln k} \simeq -5 \times 10^{-4}$ is somewhat smaller in comparison to the prediction of minimal ϕ^4 inflation. The requirement that $V^{1/4} \lesssim \Lambda$ with

$N_0 = 60$ e-foldings leads to the upper bounds $\xi \lesssim 300$ and $\lambda \lesssim 10^{-4}$ (see Fig. 4).

The inclusion of radiative corrections modifies the tree level results of nonminimal ϕ^4 inflation as follows:

$$n_s \simeq 1 - \frac{8}{3\psi^2}\left(\frac{1 + 6\kappa/\lambda(3 - 4\ln(\sqrt{\xi}\psi))}{1 - 24\kappa/\lambda\ln(\sqrt{\xi}\psi)}\right), \qquad (31)$$

$$r \simeq \frac{64}{3\psi^4}\left(\frac{1 - 6\kappa/\lambda(\psi^2 + 4\ln(\sqrt{\xi}\psi))}{1 - 24\kappa/\lambda\ln(\sqrt{\xi}\psi)}\right)^2, \qquad (32)$$

$$\frac{dn_s}{d\ln k} \simeq -\frac{32}{9\psi^4}\left(\frac{(1 + 6\kappa/\lambda(5 - 4\ln(\sqrt{\xi}\psi)))(1 - 6\kappa/\lambda(\psi^2 + 4\ln(\sqrt{\xi}\psi)))}{(1 - 24\kappa/\lambda\ln(\sqrt{\xi}\psi))^2}\right), \qquad (33)$$

with

$$\Delta_{\mathcal{R}}^2 \simeq \frac{\lambda}{\xi^2}\left(\frac{\psi^4}{768\pi^2}\right)\frac{(1 - 24\kappa/\lambda\ln(\sqrt{\xi}\psi))^3}{(1 - 6\kappa/\lambda(\psi^2 + 4\ln(\sqrt{\xi}\psi)))^2}. \qquad (34)$$

These results exhibit a reduction in the values of both r and n_s as can be seen for the curves with $\xi = 200$ in Figs. 2 and 3. In particular, for $n_s \gtrsim 0.96$ we obtain a lower bound $r \gtrsim 0.002$ (see Fig. 3). This may be compared with the result $r \gtrsim 0.02$ for the Higgs potential found in Ref. [20]. The running of the spectral index changes very slightly from $\frac{dn_s}{d\ln k} \sim -4 \times 10^{-4}$ to its tree level prediction $\frac{dn_s}{d\ln k} \sim -5 \times 10^{-4}$ within the WMAP 1-σ bounds. For $\xi = 200$ the value of ψ varies between 7 and 9. The requirement that $V^{1/4} \lesssim \Lambda$ together with the WMAP 1-σ bounds implies an upper bound $\kappa \lesssim 10^{-7}$. The limiting case $\xi \ll 1$, on the other hand, shows similar trends for the scalar spectral index and the tensor-to-scalar ratio as can be seen, for example, with the $\xi = 10^{-3}$ curves in Figs. 2 and 3.

Finally in Figs. 5 and 6 we display the predictions of nonminimal ϕ^4 inflation with the number of e-foldings $N_0 = 50$ and $N_0 = 60$. A reduction in n_s and an increase in

r is observed with a decrease in the number of e-foldings. This behavior is easy to understand with the help of analytical approximations derived in Eqs. (27) and (28). The number of e-foldings $N_0 \simeq 50$–60, depends on the reheating scenario. In our case, reheating occurs through the Yukawa coupling. Furthermore, the out of equilibrium decay of the inflaton can give rise to the observed baryon asymmetry via leptogenesis (either thermal [22] or nonthermal [23]).

To summarize, we have reconsidered nonminimal $\lambda\phi^4$ chaotic inflation and imposed the requirement that the energy scale of inflation remains below the effective UV cutoff scale, i.e., $V^{1/4} \lesssim \Lambda$. The inflaton field ϕ is a gauge singlet scalar (say axion) field. In addition to the nonminimal gravitational coupling, we have also included the Yukawa coupling of ϕ with a single right-handed neutrino, leading to radiative corrections which can have a significant effect. In the large $\xi \gg 1$ limit the requirement that $V^{1/4} \lesssim \Lambda$ provides the upper bounds $\xi \lesssim 10^2$, $\lambda \lesssim 10^{-4}$ and $\kappa \lesssim 10^{-7}$, with predictions for n_s and r that are consistent with the WMAP 1-σ bounds. For $\xi \ll 1$, we
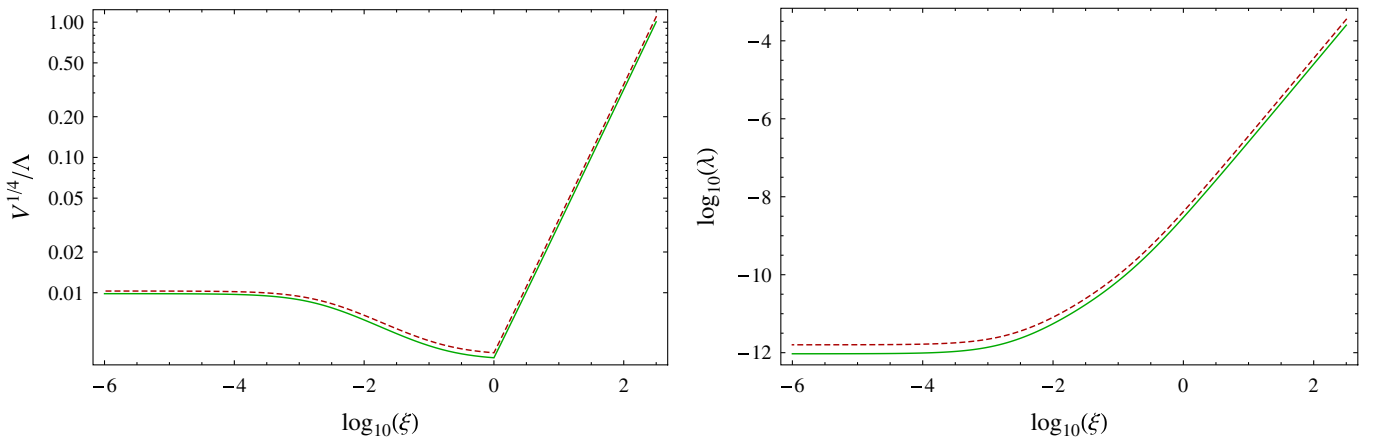

FIG. 6 (color online). $V^{1/4}/\Lambda$ and $\log_{10}(\lambda)$ vs $\log_{10}(\xi)$ for tree level ($\kappa = 0$) nonminimal ϕ^4 inflation with the number of e-foldings $N_0 = 50$ (red dashed curve) and $N_0 = 60$ (green solid curve).

obtain the lower bounds $\xi \gtrsim 10^{-3}$ and $\lambda \gtrsim 10^{-12}$ from the WMAP 1-σ bounds. Provided $n_s \geq 0.96$, we have shown that the scalar to tensor ratio $r \gtrsim 0.002$, which will soon be tested by the Planck satellite.

[1] D. S. Salopek, J. R. Bond, and J. M. Bardeen, Phys. Rev. D **40**, 1753 (1989); B. L. Spokoiny, Phys. Lett. **147B**, 39 (1984); T. Futamase and K. Maeda, Phys. Rev. D **39**, 399 (1989); R. Fakir and W. G. Unruh, Phys. Rev. D **41**, 1783 (1990); D. I. Kaiser, Phys. Rev. D **52**, 4295 (1995); E. Komatsu and T. Futamase, Phys. Rev. D **59**, 064029 (1999); K. Nozari and S. D. Sadatian, Mod. Phys. Lett. A **23**, 2933 (2008).

[2] F. L. Bezrukov, arXiv:0810.3165; F. L. Bezrukov and M. Shaposhnikov, Phys. Lett. B **659**, 703 (2008); F. L. Bezrukov, A. Magnin, and M. Shaposhnikov, Phys. Lett. B **675**, 88 (2009); F. Bezrukov, D. Gorbunov, and M. Shaposhnikov, J. Cosmol. Astropart. Phys. 06 (2009) 029; F. Bezrukov and M. Shaposhnikov, J. High Energy Phys. 07 (2009) 089; A. Anisimov, Y. Bartocci, and F. L. Bezrukov, Phys. Lett. B **671**, 211 (2009).

[3] A. O. Barvinsky, A. Y. Kamenshchik, and A. A. Starobinsky, J. Cosmol. Astropart. Phys. 11 (2008) 021; A. O. Barvinsky, A. Y. Kamenshchik, C. Kiefer, A. A. Starobinsky, and C. Steinwachs, J. Cosmol. Astropart. Phys. 12 (2009) 003; A. O. Barvinsky, A. Y. Kamenshchik, C. Kiefer, A. A. Starobinsky, and C. F. Steinwachs, arXiv:0910.1041.

[4] A. De Simone, M. P. Hertzberg, and F. Wilczek, Phys. Lett. B **678**, 1 (2009).

[5] S. C. Park and S. Yamaguchi, J. Cosmol. Astropart. Phys. 08 (2008) 009.

[6] T. E. Clark, B. Liu, S. T. Love, and T. ter Veldhuis, Phys. Rev. D **80**, 075019 (2009).

[7] R. N. Lerner and J. McDonald, Phys. Rev. D **80**, 123507 (2009).

[8] N. Okada, M. U. Rehman, and Q. Shafi, arXiv:0911.5073.

[9] M. B. Einhorn and D. R. T. Jones, J. High Energy Phys. 03 (2010) 26.

[10] C. Pallis, arXiv:1002.4765.

[11] E. Komatsu *et al.*, arXiv:1001.4538.

[12] C. P. Burgess, H. M. Lee, and M. Trott, J. High Energy Phys. 09 (2009) 103; J. L. F. Barbon and J. R. Espinosa, Phys. Rev. D **79**, 081302 (2009).

[13] C. P. Burgess, H. M. Lee, and M. Trott, J. High Energy Phys. 07 (2010) 7.

[14] M. P. Hertzberg, arXiv:1002.2995.

[15] R. N. Lerner and J. McDonald, J. Cosmol. Astropart. Phys. 04 (2010) 015.

[16] For a review and additional references, see M. Sher, Phys. Rep. **179**, 273 (1989).

[17] E. D. Stewart and D. H. Lyth, Phys. Lett. B **302**, 171 (1993).

[18] V. N. Senoguz and Q. Shafi, Phys. Lett. B **668**, 6 (2008).

[19] M. U. Rehman, Q. Shafi, and J. R. Wickman, Phys. Rev. D **79**, 103503 (2009).

[20] M. U. Rehman and Q. Shafi, Phys. Rev. D **81**, 123525 (2010).

[21] S. Tsujikawa and B. Gumjudpai, Phys. Rev. D **69**, 123523 (2004).

[22] M. Fukugita and T. Yanagida, Phys. Lett. B **174**, 45 (1986).

[23] G. Lazarides and Q. Shafi, Phys. Lett. B **258**, 305 (1991).